Article

Journal of Industrial Textiles

2016, Vol. 46(1) 59–74

DOI: 10.1177/1528083715573279
jit.sagepub.com

SAGE

Development and characterisation of antibacterial suture functionalised with N-halamines

Malik Muhammad Umair[1], Zhiming Jiang[1], Naseeb Ullah[1], Waseem Safdar[2], Zhiwei Xie[3] and Xuehong Ren[1]

Abstract

Braided and biodegradable polyglycolide suture was antibacterially functionalised with N-halamines via layer-by-layer assembly technique. Multilayers of chitosan (polycation) and poly-sodium-p-styrenesulfonate (polyanion) were successfully coated via electrostatic assembly, followed by top layer of chitosan on polyglycolide suture. Upon chlorination of coated suture with dilute sodium hypochlorite solution, the amino groups of chitosan were transformed into N-halamine structures. The transformation was assessed by iodometric/thiosulfate titration, Fourier transform infrared spectroscopy and differential scanning calorimeter analysis. The surface morphology of coated suture was observed by scanning electron microscope and atomic force microscope. Chlorine loading, antibacterial efficacy and tensile strength of chlorinated sutures treated with two different molecular weights of chitosan were compared and evaluated. A general trend of linear increase in chlorine loadings of sutures with the increase in number of layers and solution concentration was found. The chlorinated suture with high molecular weight chitosan coating completely inactivated both *Escherichia coli* O157:H7 and *Staphylococcus aureus* bacteria within 15 min of contact time. The 3T3 mouse fibroblasts *in vitro* cell cytocompatibility studies demonstrated that antibacterial sutures have fairly good biocompatibility.

[1]Key Laboratory of Eco-textiles of Ministry of Education, College of Textiles & Clothing, Jiangnan University, Wuxi, Jiangsu, China
[2]State Key Laboratory of Food Science and Technology, School of Food Science and Technology, Jiangnan University, Wuxi, Jiangsu, People's Republic of China
[3]Department of Bioengineering, University of Texas at Arlington, Arlington, Texas, USA

Corresponding author:
Xuehong Ren, Key Laboratory of Eco-textiles of Ministry of Education, College of Textiles & Clothing, Jiangnan University, Wuxi, Jiangsu 214122, China.
Email: xhren@jiangnan.edu.cn

Keywords
Layer-by-layer assembly, polyglycolide suture, antibacterial, N-halamine, chitosan, tensile, cytocompatibility

Introduction

Antibacterial surgical suture development has been under consideration from last three decades. The surface of suture exhibits an affinity for microbial adherence and potentiates surgical site infections (SSIs) [1,2]. To prevent the risk of SSIs, the implanted devices like sutures are coated with antimicrobial agents such as triclosan [3], chitosan [4], silver nanoparticles [5], antimicrobial peptides [6] and grapefruit seed extracts [7]. But these agents have some limitation depending upon their antimicrobial strength and mechanism.

Chitosan is an antimicrobial biopolymer obtained by partial N-deacetylation of chitin [8]. It is used in the medical field because of its biodegradability, biocompatibility, bioadhesivity and nontoxicity. Chitosan films have been evaluated as therapeutic wound dressing and as scaffolds for tissue and bone engineering [9–11]. To improve antimicrobial efficacy, chitosan has been chemical modified and its derivatives have shown appreciable results [12–16]. In recent studies, Cao and Sun [17] reported that incorporation of N-halamine structure in chitosan prominently enhanced its antibacterial efficacy. The N-halamine based chitosan films provided total kill of 10^8–10^9 colony forming units (CFU)/mL of Gram-negative (*E. coli*) and Gram-positive (*S. aureus*) bacteria in 10 and 60 min, respectively.

N-halamines have proven their stable, potent and durable biocidal function against a broad spectrum of microbes [18,19]. An N-halamine compound has one or more nitrogen-halogen covalent bond, formed by the halogenation of imide, amide or amino groups [20]. The mode of action is related to the release of positive chlorine from N-halamine structure that penetrates the cell wall to suitable receptors in the cells, inhibiting the cell metabolism and causing the death of microorganism [17]. N-halamine biocides are capable of killing microorganisms directly with the release of positive chlorine into the system [21]. N-halamines moieties have been introduced by different methods to produce antibacterial cellulose [22], nylon [23,24], polyester PET [25] and stainless steel [26]. In recent work of Cerkez et al. [27–29], N-halamine polyelectrolytes were synthesised and successfully coated on polypropylene and cotton fabrics via layer-by-layer (LBL) deposition method. The N-halamine polyelectrolytes provided effective inactivation of both *E. coli* and *S. aureus* bacteria. However, it was observed that to achieve the effective level of chlorine loadings, the number of multilayers were increased which alternately retarded the release of chlorine from bottom layers of the coating. For instance in the studies where a cotton sample coated with 20 bilayers provided complete inactivation of bacteria in contact time of 15 min [28]. Therefore suitable substitutes are needed to reduce the number of layers and enhance the antibacterial activity of N-halamine polyelectrolytes coating.

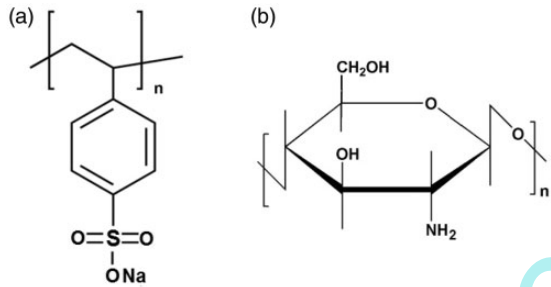

Figure 1. Chemical structures of (a) poly-sodium-p-styrenesulfonate and (b) chitosan.

In this work, N-halamine-based antibacterial polyglycolide (PGA) suture was made through LBL deposition method. The alternate polyelectrolyte layers of chitosan (polycation) and polystyrene sulphate (polyanion) were deposited on the suture, followed by a top layer of chitosan (Figure 1). The amino groups of chitosan transformed into N-halamine structures when the coated suture was chlorinated with sodium hypochlorite solution. The high-degree chemical reactive amino groups in chitosan make it a suitable candidate to use in LBL coating method. It was shown in this study that chlorinated sutures with high molecular weight (HMW) chitosan coating provided appreciable level of chlorine loadings with minimum number of layers. The deposited layers were characterised by scanning electron microscope (SEM), atomic force microscope (AFM), Fourier transform infrared (FTIR) and differential scanning calorimeter (DSC) analysis. The influence of molecular weight of chitosan and number of multilayers on chlorine content and antibacterial efficacy of chlorinated suture was evaluated. The biocompatibility of the N-halamine antimicrobial suture was assessed by a cell viability test.

Materials and methods

Materials

Chitosan of higher molecular weight (HMW, 200 kDa) and lower molecular weight (LMW, 40 KDa) with 90% deacetylation degree was bought from Zhejiang Aoxing Biochemical, China. Poly-sodium-p-styrenesulfonate (PSS) with average molecular weight 70,000 was purchased from Chengdu Chemical, China. The braided and sterilized PGA sutures were bought from Jinhuan Medical Products, China. *Staphylococcus aureus* ATCC 6538 and *Escherichia Coli* O157:H7 ATCC 43895 (American Type Culture Collection, Rockville, MD) were used in this study, and the bacteria were grown in Trypticase soy broth (TSB, Becton, Dickinson and Company Detroit, MI). Household bleach (the active chlorine content was 5%) and acetic acid (analytical grade) were purchased from Sinopharm Chemical Reagent, Shanghai, China. All reagents were used as received without further purification.

Instruments

The FTIR spectra of the treated PGA sutures were recorded by Thermo Scientific Nicolet iS10 spectrometer in the optical range of 400–4000 cm^{-1}. The DSC Q200 (TA Instruments) was used for studying the thermal behaviour of the samples. The temperature was raised from room temperature to 400 °C with heating rate of 10 °C per min under nitrogen atmosphere. Surface morphologies of uncoated and coated PGA suture were analysed by SU-1510 (Hitachi, Tokyo, Japan) field-emission SEM and CSPM-5000 (BenYuan Co. China) AFM in tapping mode equipped with silicon tip.

Preparation and coating of polyelectrolyte layers

Three different solution concentrations (1%, 2% and 3%) of HMW and LMW chitosan were prepared in aqueous acetic acid at pH 5. The solutions were stirred with a magnetic stirrer for 1 h at 60°C. The polyanionic solutions were prepared by dissolving appropriate amounts of PSS (relative to chitosan concentration) in deionized water.

In LBL coating method, suture was immersed in the HMW chitosan (polycationic) and then in the polystyrene sulphate (polyanionic) for 5 min. After adsorption of every polyion layer, the suture was rinsed with deionized water and dried at 100°C for 4 min. The desired numbers of chitosan / polystyrene sulphate (PSS) layers were deposited, followed by a top layer of chitosan. The same procedure was adopted for deposition of LMW chitosan/PSS layers on the suture samples.

Chlorination and analytical titration

To transform amino groups of chitosan into acylic N-halamines, the coated samples were chlorinated with 10% aqueous solution of household bleach (sodium hypochlorite) at pH 7 for 1 h. The samples were washed with distilled water and dried at 45 °C for 1 h to remove unreacted free chlorine from the surface of samples. The chlorine loading (Cl^+ %) on the samples was determined by iodometric/thiosulfate titration, and the chlorine loading was calculated according to equation (1)

$$Cl^+ (\%) = \frac{N \times V \times 35.45}{W \times 2} \times 100 \quad (1)$$

The Cl^+ (%) is the wt% of the oxidative chlorine on the samples; N and V are the normality (equiv/L) and volume (L) of $Na_2S_2O_3$ (titrant), respectively; and W is the weight of the suture sample in grams.

Tensile strength test of suture

Tensile strength of sutures was measured using a universal testing system (YG-B026G, China) according to ASTM D2256. The gauge length used was

50 mm, and the extension rate was 200 mm/min. The tests were carried out under a standard atmosphere for textile testing (T: $20 \pm 2^{\circ}C$, RH: $65 \pm 2\%$), and each sample was tested three times. The straight-pull and knot-pull strength tests were performed for untreated, unchlorinated and chlorinated sutures. In straight-pull test, the suture was clamped in between the fixed jaw and moving jaw of the tensile tester, and pulled until they broke. However, for the knot-pull test, the suture material was tied into a square knot by single throw around a 6-mm diameter rod. The rod was removed and the ends of the suture were positioned around the grip mandrels such that the knot was at the centre of the gauge area. The relationship between the tensile strength of unknotted and knotted suture, which is designated as relative knot security (RKS) [30], was measured by the following equation

$$\text{Relative Knot Security } (\%) = \frac{\text{Tensile strength of knotted suture}}{\text{Tensile strength of unknotted suture}} \times 100 \quad (2)$$

Antibacterial efficacy test

The antimicrobial properties of unchlorinated and chlorinated sutures were evaluated by modified test method. The *S. aureus* (ATCC 6538) and *E. coli* O157:H7 (ATCC 43895) were prepared in sterile 100 µM phosphate buffer to produce a suspension of 10^6 CFU/mL. The samples of 1 g were challenged for 15, 30 and 60 min with 200 µL bacterial suspensions. Then the samples were quenched with 10.0 mL solution of 0.02 N sodium thiosulfate to neutralize the oxidative chlorine and vortexed for 1 min. Serial dilutions of the quenched solution samples were made using 100 µM phosphate buffer (pH 7) and plated on Trypticase agar. After incubation for 24 h at 37 °C, the viable bacterial colonies were recorded for biocidal efficacy analysis.

In vitro cytocompatibility test

The cytocompatibility of N-halamine modified suture was evaluated *in vitro* by using NIH 3T3 mouse fibroblasts. Briefly, 3T3 cells were cultured in Dulbecco's modified eagle medium (DEME) with 10% fetal bovine serum (FBS) and 1% Penicillin Streptomycin (Pen Strep) at 37 °C with 95% humidity and 5% CO_2; 10,000 cells in 200 µL DMEM were seeded into each well of a 98-well plate. After cells adhered to the plate, a piece of suture fibre 1 cm long was placed in each well, followed by 24 h incubation. After 24 h, a Cell Counting Kit-8 (CCK8) assay was performed to determine the cell viability. The tissue culture plate itself was served as the control. The cell viability was reported as the percentage to the control ($n = 6$ for all samples).

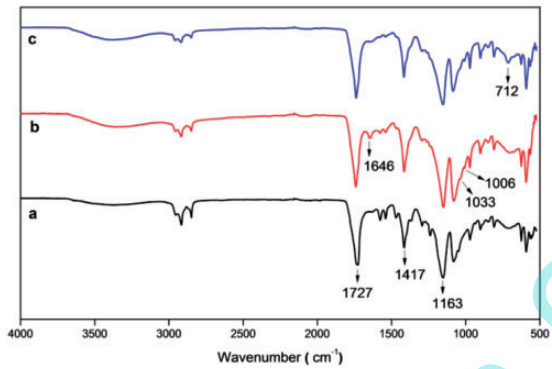

Figure 2. FTIR spectra of (a) untreated suture, (b) unchlorinated and (c) chlorinated HMW CS/PSS sutures.

Results and discussions

FTIR characterisation of LBL coatings

The FTIR spectra of PGA sutures coated with multilayers of HMW-chitosan/PSS and LMW-chitosan/PSS were observed in Figures 2 and 3, respectively. The spectrum of PGA suture showed the absorption bands at around 2960 cm^{-1} (γ−CH), 2882 cm^{-1} (−CH2), 1417 cm^{-1} (δ−CH), 1163 cm^{-1} and 1090 cm^{-1} (γ−C−O), and the group of bands in the region of 1000–800 cm^{-1} was possibly due to a mix of vibrational modes of $[-C-C-]_n$ repeat units and −CH twist. Also the strong band at 1725 cm^{-1} is characteristic of [C=O stretching] groups [31].

In the spectrum of LBL-coated PGA suture, the presence of chitosan was demonstrated by characteristics peaks at 1652–1646 cm^{-1} (N–H bending vibrations) [32]. Moreover, 3350 cm^{-1} region is donated by stretching vibration for O–H, the extension vibration of N–H and inter-molecular hydrogen bonds of the polysaccharides. The presence of PSS chains was shown in the spectra by following characteristics bands: 1037 cm^{-1} assigned to the S=O symmetrical stretching vibrations and the peak at 1008 cm^{-1} was attributed to aromatic in-plane vibration [33,34]. In the spectra of coated sutures after chlorination new peaks were recorded at 717–712 cm^{-1} (see Figures 2 and 3). These peaks were assigned as N-Cl bond formation, as previously observed elsewhere [35]. It was also seen that finger print region observed in pure PGA spectrum from 1163 to 1650 cm^{-1} was diminished in spectrum of chlorinated suture. All the above-mentioned bands were same for both HMW and LMW chitosan/PSS-coated sutures spectra (Figure 3) as the backbone was PGA.

To further confirm the chlorination of chitosan, FTIR spectra of pure chitosan and chlorinated chitosan were recorded in Figure 4. The new peaks were observed at 3295 and 721 cm^{-1} in chlorinated chitosan. These peaks were assigned as the secondary amine group and an organic halogen formed, respectively [35,36].

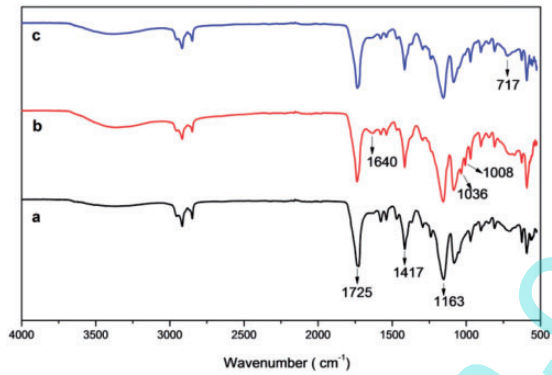

Figure 3. FTIR spectra of (a) untreated suture, (b) unchlorinated and (c) chlorinated LMW chitosan/PSS sutures.

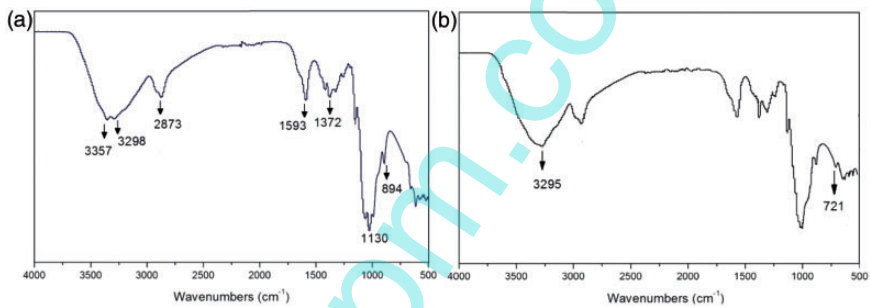

Figure 4. FTIR of (a) pure chitosan and (b) chlorinated chitosan.

Chlorine content of suture

Deposition of the polyelectrolytes was further affirmed by measuring the chlorine loadings of the chlorinated sutures having different layers and concentration of chitosan/PSS solutions. A linear increase in chlorine loadings with respect to the increasing number of layers and solution concentration was obtained indicating a direct correlation between variables.

As seen in Figure 5, LBL coatings on suture by HMW chitosan showed higher chlorine loadings than LMW chitosan. The greater mobility and ionic interaction of small chains and large active surface area of LMW chitosan than long-chained HMW chitosan thereby facilitated more bond formation with polyanions [37,38]. As a result less number of free amino groups is available in LMW chitosan as compared to HMW chitosan. This may cause limited transformation of amino groups into N-halamine structures and hence leading to lower chlorine loadings of LMW chitosan LBL coatings. Moreover, N-halamine-modified chitosan coatings provided high chlorine loadings with far less multilayers when compared with N-halamine polyelectrolytes synthesised in former studies [27–29].

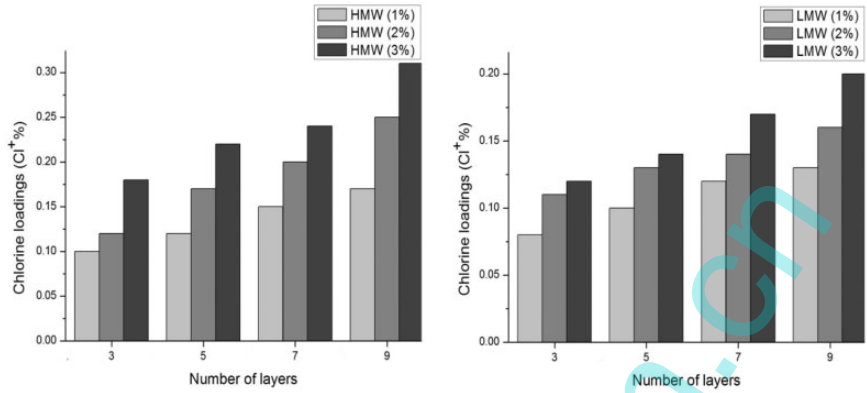

Figure 5. Effect of concentration and molecular weight of chitosan, and number of layers on chlorine loadings of sutures.

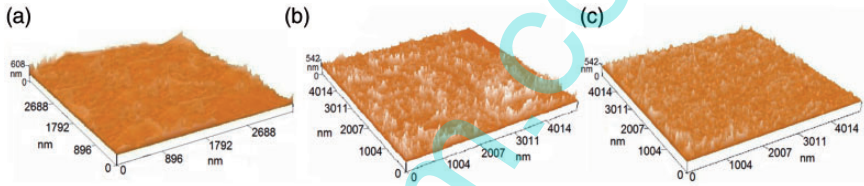

Figure 6. 3D AFM images of (a) untreated suture, (b) LMW chitosan/PSS and (c) HMWchitosan/PSS-coated sutures.

AFM analysis of coatings

The surface topography was conducted on PGA suture by AFM microscopy in order to point out the morphological change obtained after the LBL deposition of HMW chitosan/PSS and LMW chitosan/PSS. In Figure 6(a) the surface of untreated PGA analysis showed a smooth surface. In Figure 6(b) the surface of LMW chitosan-coated suture showed rough and agglomerated layer. This agglomeration was possible because of strong interaction of amine groups of LMW chitosan and sulphonate groups of PSS. Contrarily to LMW chitosan/PSS, the topography of HMW chitosan/PSS-treated suture in Figure 6(c) revealed a non-uniform but micro-structural and less agglomerated layer.

SEM analysis of coatings

The SEM was employed to image the surface of uncoated and coated suture at ×3000 magnification. In Figure 7(a), a neat surface of untreated PGA suture is shown. Comparatively a more rough and agglomerated coating of LMW chitosan/PSS than HMW chitosan/PSS on suture was recorded in

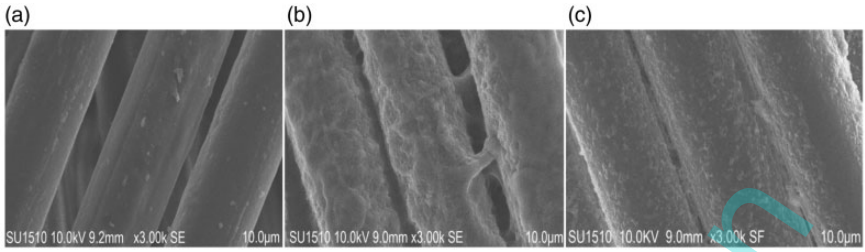

Figure 7. SEM images of (a) untreated suture, (b) LMW chitosan/PSS and (c) HMW chitosan/PSS coated sutures.

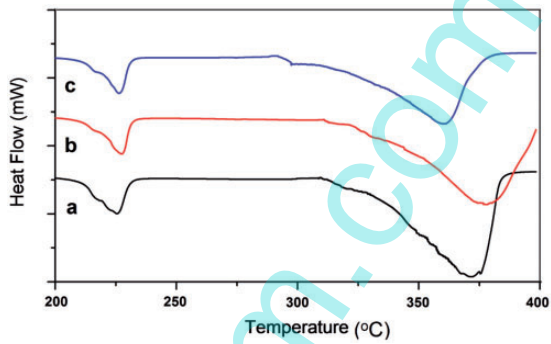

Figure 8. DSC curves of (a) untreated suture, (b) unchlorinated and (c) chlorinated sutures.

Figure 7(b) and (c), respectively. The SEM images of LMW chitosan/PSS- and HMW chitosan/PSS-coated sutures showed coatings of similar characteristics as observed in the AFM topographies, which can be easily recognised in Figure 6.

The surface analysis achieved by AFM and SEM demonstrated that the HMW chitosan/PSS-coated suture has uniform and compact coating as compared to LMW chitosan/PSS-coated suture.

DSC analysis

The DSC results of the samples are displayed in Figure 8. As in this figure, the DSC scan of untreated PGA showed an endothermic peak at 224 °C representing melting point of the PGA [39]. And when comparing to DSC scans of unchlorinated and chlorinated sutures, this first peak shifted to slightly higher temperatures. There was also another endothermic event at 371°C in the thermogram of untreated PGA. This peak was shifted to 379°C in unchlorinated and to 360°C in chlorinated suture. In the DSC curve of the chlorinated suture, a new endothermic peak was also recorded at 295°C, as observed in former studies [17].

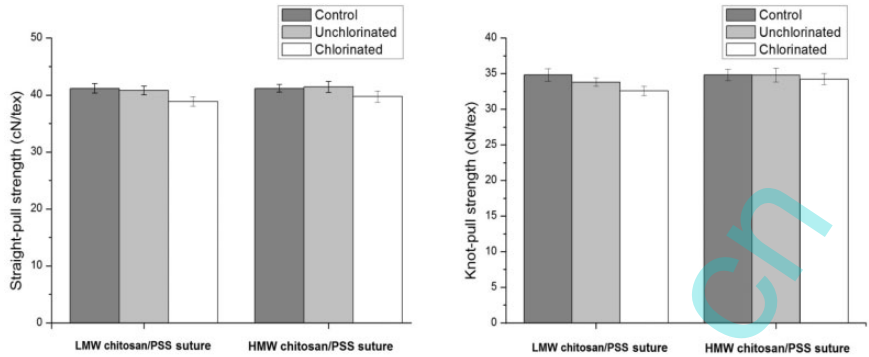

Figure 9. Straight-pull and knot-pull strengths of suture before and after chlorination.

Tensile properties of sutures

The tensile strength of surgical suture is very important. However, for security of suturing in surgical use, knot-pull strength is generally more vital. In straight-pull test, HMW chitosan/PSS-coated sutures endured better tensile strength than that of LMW chitosan/PSS, as graphically represented in Figure 9. And in knot-pull strength test, generally a slight decrease in strength of coated sutures was recorded when compared with untreated sutures. In Figure 9, it was observed that force necessary to break a knotted suture was lower than that required to break an untied suture made of the same material [30]. This confirmed the fact that when external force was applied on a knotted suture, the site of breakage was the knot itself; indicating knot being a weakest part of suture when subjected to tension [4]. Furthermore, the knot security of suture after chlorination treatment was investigated by mathematical equation (2). It was recorded that HMW chitosan/PSS and LMW chitosan/PSS chlorinated sutures exhibited 86.13% and 83.84% RKS, respectively, against 84.57% RKS of control sample. These relatively better tensile properties of HMW chitosan-coated suture were due to the longer polymer chains resulting in better binding of fibres in the braided suture.

The overall trend of slight decrease in tensile strength was observed after chlorination (see Figure 9). It could be due to degradation of ester linkages of PGA suture by strong oxidising nature of chlorinating agent (NaOCl). But this decrease of tensile strength is insignificant to vary the tensile properties of sutures.

Antibacterial efficacy test

The sutures coated with HMW chitosan/PSS and LMW chitosan/PSS were challenged with *S. aureus* and *E. coli* O157:H7 by a modified antibacterial susceptibility test. The unchlorinated sutures were used as control. The results, shown in Table 1, revealed the antibacterial properties of unchlorinated and chlorinated sutures. It was observed that bacterial reduction of unchlorinated suture was insignificant, as expected. The unchlorinated HMW chitosan/PSS suture showed highest value of

Table 1. Antibacterial efficacy test.

Samples	Contact time (min)	Bacterial reduction (log)	
		S. aureus[a]	*E. coli*[b]
HMW-LBL (Control)	30	0.03	0.02
HMW-LBL (Chlorinated)	15	5.62	5.93
	30	5.62	5.93
	60	5.62	5.93
LMW-LBL (Control)	30	0.06	0.04
LMW-LBL (Chlorinated)	15	2.31	1.57
	30	5.62	5.93
	60	5.62	5.93

HMW: high molecular weight; LBL: layer-by-layer; LMW: low molecular weight.
[a]The inoculum concentrations were 5.62 logs.
[b]The inoculum concentrations were 5.93 logs.

bacterial log reduction (0.03 log of *S. aureus* and 0.02 log of *E. coli*) in 30-min contact. The inactivation of bacteria was mainly related with increase in number of free amino groups of chitosan [40]. Generally, the unchlorinated sutures were having high inhibitory activity against Gram-positive bacteria (*S. aureus*) than Gram-negative bacteria (*E. coli*), as similarly recorded in previous studies [40,41]. On the contrary, the chlorinated sutures provided rapid inactivation of both *S. aureus* and *E. coli*. The chlorinated HMW chitosan/PSS suture (0.31 Cl^+ %) showed complete inactivation of bacteria (5.62 log reduction of *S. aureus* and 5.93 log reduction of *E. coli*) in 15 min contact time. LMW chitosan/PSS suture (0.20 Cl^+ %) exhibited total inactivation of bacteria within 30 min contact time. Clearly, the chlorinated suture was effective in complete deactivation of all the inoculated bacteria than unchlorinated suture as seen in Figure 10. The antibacterial efficacy was improved due to the oxidative chlorine released from the N-halamines causing the expiration of bacteria [42]. N-halamines-modified chitosan prepared via chlorination treatment provided the biocidal properties, as seen in the former studies [17]. Thus N-halamines-based suture can give rapid and effective inactivation of colonisation of both Gram-positive (*S. aureus*) and Gram-negative (*E. coli*) bacteria on its surface.

In-vitro cytocompatibility test

The *in vitro* cytocompatibility was determined by incubating sutures within the media of mouse 3T3 fibroblasts for 24 h. As shown in Figure 11, untreated suture and LBL-coated suture exhibited no toxicity with about 100% cells being viable and no significant difference to control ($p > 0.05$). Thus, the LBL coating containing

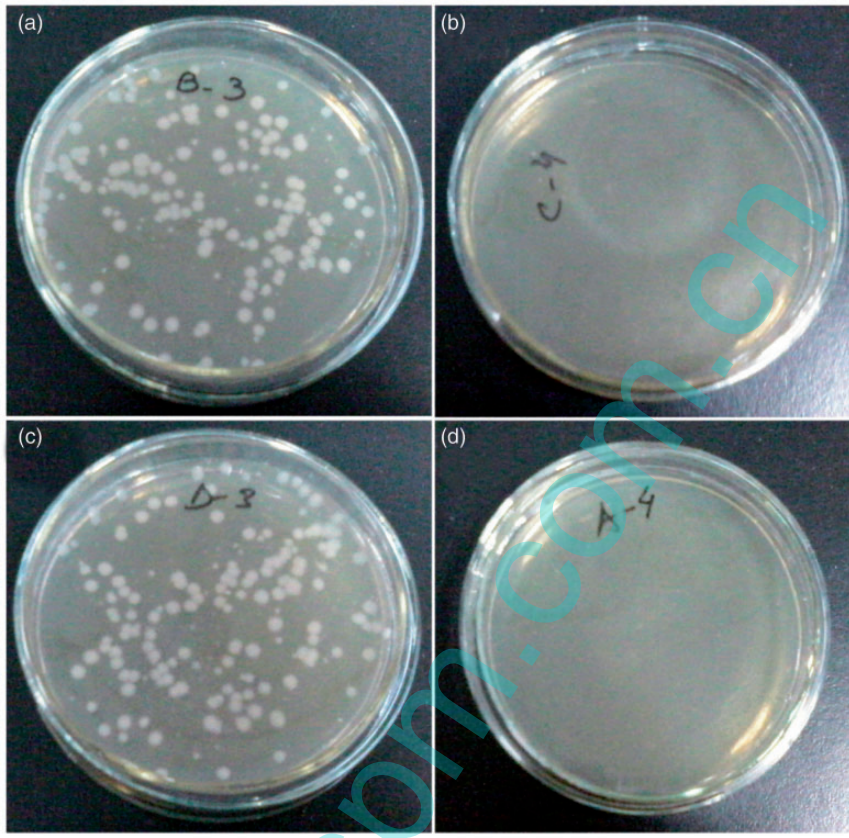

Figure 10. Plates with *E. coli* colonies for (a) unchlorinated and (b) chlorinated sutures, and *S. aureus* colonies for (c) unchlorinated and (d) chlorinated sutures. The challenge time was 15 min.

chitosan and PSS was not toxic to cells *in vitro*. However, after chlorination, the suture with chlorine loading of 0.31 wt% showed some toxicity of about 72% cell viability, which was significantly lower than that of the control ($p < 0.05$). The result is consistent with the previous findings that chlorinated materials caused significant decrease in cell viability [43,44]. But it is also observed in previous studies that the consumption of oxidative chlorine with time promoted the cell growth. The cell viability is greatly affected if the test sample has high amount of chlorine loading (Cl^+ %). However, the availability of the antimicrobial N-halamine functionalized suture will need to be determined by *in vivo* studies in the future.

Conclusions

PGA suture was successfully coated with chitosan/PSS by LBL deposition method. A linear relation was obtained between the number of layers and chlorine loadings

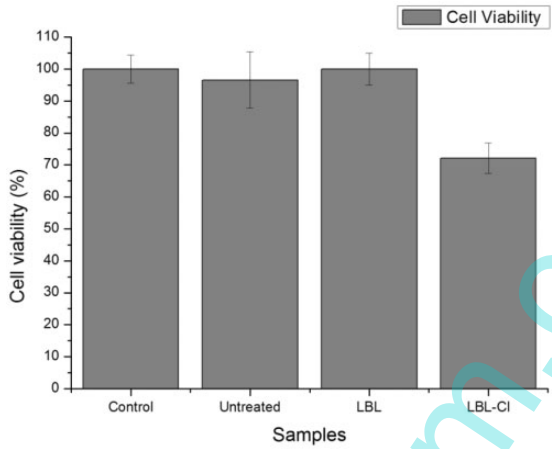

Figure 11. 3T3 mouse fibroblast viability after incubated with different sutures for 24 h. Blank tissue culture plate was the control (*, $p < 0.05$).

on the suture. The antibacterial efficacy was improved when amino groups of chitosan were transformed into N-halamines structures. The chlorinated suture with HMW chitosan coating outperformed the LMW chitosan in antibacterial and tensile properties. The most effective biocidal coating was obtained with nine layers of chlorinated HMW chitosan killing all the bacteria (*E. coli* and *S. aureus*) within 15 min contact time. Therefore, N-halamine-based sutures can reduce the risk of SSI. It was deduced that LBL method was useful in surface modification of PGA, as intrinsic tensile properties of PGA sutures were not altered significantly. The rapid disinfection by chitosan coating based on N-halamines can find many uses in biocompatible and antibacterial functionalisation of medical devices.

Declaration of Conflicting Interests

The author(s) declared no potential conflicts of interest with respect to the research, authorship, and/or publication of this article.

Funding

The author(s) disclosed receipt of the following financial support for the research, authorship, and/or publication of this article: This research was financially supported by the Project for Jiangsu Scientific and Technological Innovation Team, the National Thousand Young Talents Program and the Scientific Research Foundation for Returned Overseas Chinese Scholars, Ministry of Education China.

References

[1] Edmiston CE, Seabrook GR, Goheen MP, et al. Bacterial adherence to surgical sutures: Can antibacterial-coated sutures reduce the risk of microbial contamination? *J Am Coll Surg* 2006; 203: 481–489.

[2] Katz S, Izhar M and Mirelman D. Bacterial adherence to surgical sutures: A possible factor in suture induced infection. *Ann Surg* 1981; 194: 35–41.
[3] Gomez-Alonso A, Garcia-Criado FJ, Parreno-Manchado FC, et al. Study of the efficacy of Coated VICRYL plus antibacterial suture (coated polyglactin 910 suture with Triclosan) in two animal models of general surgery. *J Infect* 2007; 54: 82–88.
[4] Viju S and Thilagavathi G. Effect of chitosan coating on the characteristics of silk-braided sutures. *J Ind Text* 2013; 42: 256–268.
[5] Cao G-F, Sun Y, Chen J-G, et al. Sutures modified by silver-loaded montmorillonite with antibacterial properties. *App Clay Sci* 2014; 93–94: 102–106.
[6] Li Y, Kumar KN, Dabkowski JM, et al. New bactericidal surgical suture coating. *Langmuir* 2012; 28: 12134–12139.
[7] Lee HS, Park SH, Lee JH, et al. Antimicrobial and biodegradable PLGA medical sutures with natural grapefruit seed extracts. *Mater Lett* 2013; 95: 40–43.
[8] Park SY, Marsh KS and Rhim JW. Characteristics of different molecular weight chitosan films affected by the type of organic solvents. *J Food Sci* 2002; 67: 194–197.
[9] Xu H, Ma L, Shi H, et al. Chitosan–hyaluronic acid hybrid film as a novel wound dressing: *In vitro* and *in vivo* studies. *Polym Adv Technol* 2007; 18: 869–875.
[10] Peh K, Khan T and Ch'ng H. Mechanical, bioadhesive strength and biological evaluations of chitosan films for wound dressing. *J Pharm Pharm Sci* 2000; 3: 303–311.
[11] Li Z, Ramay HR, Hauch KD, et al. Chitosan–alginate hybrid scaffolds for bone tissue engineering. *Biomaterials* 2005; 26: 3919–3928.
[12] Hsieh W-C, Chang C-P and Lin S-M. Morphology and characterization of 3D microporous structured chitosan scaffolds for tissue engineering. *Colloids Surf B* 2007; 57: 250–255.
[13] Cheng X, Ma K, Li R, et al. Antimicrobial coating of modified chitosan onto cotton fabrics. *App Surf Sci* 2014; 309: 138–143.
[14] Li R, Hu P, Ren X, et al. Antimicrobial N-halamine modified chitosan films. *Carbohydr Polym* 2013; 92: 534–539.
[15] Huh MW, Kang I-K, Lee DH, et al. Surface characterization and antibacterial activity of chitosan-grafted poly(ethylene terephthalate) prepared by plasma glow discharge. *J App Polym Sci* 2001; 81: 2769–2778.
[16] Mohamed NA, Sabaa MW, El-Ghandour AH, et al. Quaternized N-substituted carboxymethyl chitosan derivatives as antimicrobial agents. *Int J Biol Macromol* 2013; 60: 156–164.
[17] Cao Z and Sun Y. N-halamine-based chitosan: Preparation, characterization, and antimicrobial function. *J Biomed Mater Res A* 2008; 85: 99–107.
[18] Liang J, Wu R, Wang JW, et al. N-halamine biocidal coatings. *J Ind Microbiol Biotechnol* 2007; 34: 157–163.
[19] Cerkez I, Kocer HB, Worley SD, et al. N-halamine copolymers for biocidal coatings. *React Funct Polym* 2012; 72: 673–679.
[20] Jiang Z, Ma K, Du J, et al. Synthesis of novel reactive N-halamine precursors and application in antimicrobial cellulose. *App Surf Sci* 2014; 288: 518–523.
[21] Barnela SB, Worley SD and Williams DE. Syntheses and antibacterial activity of new N-halamine compounds. *J Pharm Sci* 1987; 76: 245–247.
[22] Sun Y and Sun G. Novel regenerable N-halamine polymeric biocides. I. Synthesis, characterization, and antibacterial activity of hydantoin-containing polymers. *J App Polym Sci* 2001; 80: 2460–2467.

[23] Chu CC, Tsai WC, Yao JY, et al. Newly made antibacterial braided nylon sutures. I. *In vitro* qualitative and *in vivo* preliminary biocompatibility study. *J Biomed Mater Res* 1987; 21: 1281–1300.
[24] Lin J, Winkelman C, Worley SD, et al. Antimicrobial treatment of nylon. *J App Polym Sci* 2001; 81: 943–947.
[25] Ren X, Kocer HB, Kou L, et al. Antimicrobial polyester. *J App Polym Sci* 2008; 109: 2756–2761.
[26] Bastarrachea LJ and Goddard JM. Development of antimicrobial stainless steel via surface modification with N-halamines: Characterization of surface chemistry and N-halamine chlorination. *J App Polym Sci* 2013; 127: 821–831.
[27] Cerkez I. Rapid disinfection by N-halamine polyelectrolytes. *J Bioact Compat Polym* 2013; 28: 86–96.
[28] Cerkez I, Kocer HB, Worley SD, et al. N-Halamine biocidal coatings via a layer-by-layer assembly technique. *Langmuir* 2011; 27: 4091–4097.
[29] Cerkez I, Worley SD, Broughton RM, et al. Antimicrobial surface coatings for polypropylene nonwoven fabrics. *React Funct Polym* 2013; 73: 1412–1419.
[30] Thacker JG, Rodeheaver G, Moore JW, et al. Mechanical performance of surgical sutures. *Am J Surg* 1975; 130: 374–380.
[31] Hajiali H, Shahgasempour S, Naimi-Jamal MR, et al. Electrospun PGA/gelatin nanofibrous scaffolds and their potential application in vascular tissue engineering. *Int J Nanomed* 2011; 2011: 2133–2141.
[32] Gregorio-Jauregui KM, Pineda MG, Rivera-Salinas JE, et al. One-step method for preparation of magnetic nanoparticles coated with chitosan. *J Nanomater* 2012; 2012: 8.
[33] Yu J, Yi B, Xing D, et al. Degradation mechanism of polystyrene sulfonic acid membrane and application of its composite membranes in fuel cells. *Phys Chem Chem Phys* 2003; 5: 611–615.
[34] Su N, Li HB, Zheng HM, et al. Synthesis and characterization of poly(sodium-p-styrenesulfonate)/modified SiO_2 spherical brushes. *eXPRESS Polym Lett* 2012; 6: 680–686.
[35] Kador KE and Subramanian A. Selective modification of chitosan to enable the formation of chitosan-DNA condensates by electron donator stabilization. *Int J Carbohydr Chem* 2011; 2011: 11.
[36] Mohan J. *Organic spectroscopy: Principles and applications*. CRC Press LLC, Alpha Science International Ltd. Harrow, U.K., 2004.
[37] Chattopadhyay DP and Inamdar MS. Aqueous behaviour of chitosan. *Int J Polymer Sci* 2010; 2010: 7.
[38] Liu Z, Ge X, Lu Y, et al. Effects of chitosan molecular weight and degree of deacetylation on the properties of gelatine-based films. *Food Hydrocolloids* 2012; 26: 311–317.
[39] Ramdhanie LI, Aubuchon SR, Boland ED, et al. Thermal and mechanical characterization of electrospun blends of poly(lactic acid) and poly(glycolic acid). *Polym J* 2006; 38: 1137–1145.
[40] Thayza Christina Montenegro S, Thatiana Montenegro S-A, Horacinna Maria de Medeiros C, et al. Microbiological chitosan: Potential application as anticariogenic agent. *Pract Appl Biomed Eng* 2013; C9: 230–244.
[41] No HK, Young Park N, Ho Lee S, et al. Antibacterial activity of chitosans and chitosan oligomers with different molecular weights. *Int J Food Microbiol* 2002; 74: 65–72.

[42] Ahmed AE-SI, Wardell JN, Thumser AE, et al. Metabolomic profiling can differentiate between bactericidal effects of free and polymer bound halogen. *J App Polym Sci* 2011; 119: 709–718.
[43] Li R, Dou J, Jiang Q, et al. Preparation and antimicrobial activity of β-cyclodextrin derivative copolymers/cellulose acetate nanofibers. *Chem Eng J* 2014; 248: 264–272.
[44] Ma K, Liu Y, Xie Z, et al. Synthesis of novel N-Halamine epoxide based on cyanuric acid and its application for antimicrobial finishing. *Ind Eng Chem Res* 2013; 52: 7413–7418.